[30] Thornton, J. A., "Comparison of Theory and Experiment for Ion Collection by Spherical and Cylindrical Probes in a Collisional Plasma," *AIAA Journal*, Vol. 9, No. 2, Feb. 1971, pp. 342–344.

[31] Inutake, M. and Kuriki, K., "Characteristics of Cylindrical Langmuir Probe with the Effect of Collision," *Book of Abstracts, 8th Rarefied Gas Dynamics Symposium*, Stanford Univ., Stanford, Calif. 1972.

[32] Su, C. S. and Lam, S. H., "Continuum Theory of Spherical Electrostatic Probes," *The Physics of Fluids*, Vol. 6, No. 10, Oct. 1963, pp. 1479–1491.

[33] Peterson, E. W., "Electrostatic Probe Electron Current Collection in the Transition Regime," *AIAA Journal*, Vol. 9, No. 7, July 1971, pp. 1404–1405.

[34] Hester, S. D. and Sonin, A. A., "Ion Temperature Sensitive End Effect in Cylindrical Langmuir Probe Response at Ionospheric Satellite Conditions," *The Physics of Fluids*, Vol. 13, No. 5, May 1970, pp. 1265–1274.

[35] Graf, K. A. and De Leeuw, J. H., "Comparison of Langmuir Probe and Microwave Diagnostic Techniques," *Journal of Applied Physics*, Vol. 38, No. 11, Oct. 1967, pp. 4466–4472.

[36] Bettinger, R. T. and Chen, A. A., "An End Effect Associated with Cylindrical Langmuir Probes Moving at Satellite Velocities," *Journal of Geophysical Research*, Vol. 73, No. 7, April 1968, pp. 2513–2528.

[37] Hester, S. D. and Sonin, A. A., "Some Results from a Laboratory Study of Satellite Wake Structure and Probe Response in Collisionless Plasma Flows," *Rarefied Gas Dynamics*, 6th Symposium, Vol. 2, Academic Press, New York, 1969, p. 1659.

[38] Sanmartin, J. R., "Ion Temperature-Sensitive Effect in Transient Langmuir Probe Response," *The Physics of Fluids*, Vol. 15, No. 3, March 1972, pp. 391–401.

[39] Sanmartin, J. R., "End Effects in Langmuir Probe Response under Ionospheric Satellite Conditions," Pub. 71-8, 1971, MIT Fluid Mechanics, Lab., Cambridge, Mass.

[40] Jakubowski, A. K., Effect of Angle of Incidence on the Response of Cylindrical Electrostatic Probes at Supersonic Speeds," *AIAA Journal*, Vol. 10, No. 8, Aug. 1972, pp. 988–995.

[41] Clayden, W. A., "Langmuir Probe Measurements in the R.A.R.D.E. Plasma Jet," *Rarefied Gas Dynamics*, 3rd Symposium, Vol. II, Academic Press, New York, 1963, p. 435.

[42] Smetana, F. O., "On the Current Collected by a Charged Circular Cylinder Immersed in a Two-Dimensional Rarefied Plasma Stream," *Proceedings of the 3rd Rarefied Gas Dynamics Symposium*, Vol. II, edited by J. Laurmann, Academic Press, New York, 1963, pp. 65–92.

[43] Kanal, M., "Theory of Current Collection of Moving Cylindrical Probes," *Journal of Applied Physics*, Vol. 35, No. 6, June 1964, pp. 1697–1703.

[44] Tan, W. P. S., "Transverse Cylindrical Probe in Plasma Diagnostics," *Journal of Physics D: Applied Physics*, Vol. 6, 1973, pp. 1206–1216 (Great Britain).

[45] Kang, S. W., Jones, L. W., and Dunn, M. G., "Theoretical and Measured Electron Density Distributions at High Altitudes," *AIAA Journal*, Vol. 11, No. 2, Feb. 1973, pp. 141–149.

[46] Koopman, D. W., "Langmuir Probe and Microwave Measurements of the Properties of Streaming Plasmas Generated by Focused Laser Pulses," *The Physics of Fluids*, Vol. 14, No. 8, Aug. 1971, pp. 1707–1716.

[47] Koopman, D. W. and Segall, S. B., "Application of Cylindrical Langmuir Probes to Streaming Plasma Diagnostics," *The Physics of Fluids*, Vol. 16, No. 7, July 1973, pp. 1149–1156.

[48] Fournier, G., "Écoulement de Plasma sans Collisions Autour d'un Cylindre en Vue d'Applications Aux Sondes Ionosphériques," ONERA Publication 137, 1971, Chatillon, France; see also Taillet, J., Brunet, A., and Fournier, G., "Behavior of a Positive Probe in High Speed Collision-Free Plasma Flow," *Dynamics of Ionized Gases*, edited by M. J. Lighthill, I. Imai, and H. Sato, Halstead Press, Wiley, New York, 1973, pp. 317–328.

[49] Sonin, A. A., "Theory of Ion Collection by a Supersonic Atmospheric Sounding Rocket," *Journal of Geophysical Research*, Vol. 72, No. 17, Sept. 1967, pp. 4547–4557.

[50] Parker, L. W. and Whipple, E. C., Jr., "Theory of a Satellite Electrostatic Probe," *Annals of Physics*, Vol. 44, 1967, pp. 126–161.

[51] Parker, L. W. and Whipple, E. C., Jr., "Theory of Spacecraft Sheath Structure, Potential and Velocity Effects on Ion Measurements by Traps and Mass Spectrometers," *Journal of Geophysical Research*, Vol. 75, 1970, pp. 4720–4733.

[52] Whipple, E. C. Jr. and Parker, L. W., "Theory of an Electron Trap on a Charged Spacecraft," *Journal of Geophysical Research*, Vol. 74, 1969, pp. 2962–2971.

FEBRUARY 1974 AIAA JOURNAL VOL. 12, NO. 2

Part 2. Continuum Probes

Introduction

THE effects of collisions in the sheath formed around an electrostatic probe were discussed in some detail in part 1 of this survey paper. In part 2, we will review the status of continuum electrostatic probes which represent the limit of "many collisions" within the sheath. As outlined in the Introduction of part 1, one can identify two regimes of continuum probe operation and one hybrid case depending on the relative magnitude of smallest mean-free-path λ and the Debye length λ_D. These are: $L \gg \lambda_D \gg \lambda$—collisional thin sheath; $\lambda_D \geqq L \gg \lambda$—collisional thick sheath; and $L \gg \lambda \geqq \lambda_D$—collisionless thin sheath (dense case). Here L is a characteristic length particular to the problem at hand. The last regime is the hybrid case (sometimes alluded to as the dense case) where the sheath can be described by the collisionless considerations discussed in part 1, but the motion of carriers in the bulk of the plasma is determined from the continuum flow equations. The first two are collision-dominated throughout the plasma and the motion of the carriers is determined by processes of convection, diffusion, and mobility, governed by the continuum equations, Eqs. (1–4).

In part 2 we will discuss the first two regimes in detail. The third will be mentioned briefly. We will develop expressions for probe current collection where possible, display numerical solutions for probe characteristics and make comparison with experimental data where such data exist.

We will limit our discussion to weakly ionized plasmas which will enable us to decouple the fluid mechanical from the electrical characteristics of the flow. The gas velocity, density, and temperature fields are, therefore, presumed to be known and the quantities to be determined are charged particle densities, the electric field in the plasma, and the electron temperature. A brief mention will be made of special probe topics which deal with surface phenomena and turbulent plasmas.

Part 2 Some Physical Considerations

The relative importance of convection, diffusion, mobility, and charge generation on current collection are determined by nondimensional parameters that arise naturally, by nondimensionalizing Eqs. (1–4) as will be shown later on. To put the

problem in perspective, however, we will discuss in broad terms some of these parameters.

As with free-molecule and transitional electrostatic probes, there are two general plasma states encountered in continuum probe operations, the quiescent plasma and the flowing plasma (laminar or turbulent). These are determined by the magnitude of the convective terms in the governing charged particle conservation equations. The nondimensional parameter here is the electric Reynolds number which is the product of the ion Schmidt number and the flow Reynolds number ($ReSc_i$).

When $Re\,Sc_i \ll 1$ we have the quiescent plasma case, in which convective effects can be neglected. Convection must be included when $Re\,Sc_i$ is non-negligible. The usual boundary-layer type approximations can be employed when $Re\,Sc_i \gg 1$. All available analyses are for either the negligible or the large ($Re\,Sc_i \gg 1$) convection limits.

For either of the abovementioned quiescent or large convective cases, the plasma may be incompressible with constant properties or it may be compressible with variable properties. Whether compressible or incompressible, the plasma can have two limiting chemical or thermal states. These states are governed by the appropriate Damkohler numbers which will be discussed later.

The next subdivision is that of thin or thick sheath. By "thin" sheath, it is implied here that the sheath is sufficiently thin such that its effect on the rest of the plasma is negligible. All other sheaths are referred to as "thick" sheaths.

Governing Equations

The governing equations that describe the continuum probe operation in weakly ionized plasmas consist of the species continuity equations, the electron-energy equation, and the Poisson equation.* By choosing a set of reference quantities we can nondimensionalize the governing equations, viz., $\tilde{\mathbf{u}} = \mathbf{u}/u_o$, $\tilde{\rho} = \rho/\rho_o$, $\tilde{\nabla} = L\nabla$, $\tilde{T} = T/T_o$, etc., and obtain the following:

Ion Conservation

$$(Re\,Sc_i)\tilde{\rho}\tilde{\mathbf{u}}\cdot\tilde{\nabla}\tilde{C}_i - \tilde{\nabla}\cdot\left[\tilde{\rho}\tilde{D}_i\left(\frac{\tilde{C}_i}{\tilde{p}_i}\tilde{\nabla}\tilde{p}_i - Z\frac{\chi_p\tau}{\tilde{T}_i}\tilde{C}_i\tilde{\nabla}\psi\right)\right] = \mathscr{D}\tilde{w}_i \quad (1)$$

Electron Conservation

$$(\beta\,Re\,Sc_i)\tilde{\rho}\tilde{\mathbf{u}}\cdot\tilde{\nabla}\tilde{C}_e - \tilde{\nabla}\cdot\left[\tilde{\rho}\tilde{D}_e\left(\frac{\tilde{C}_e}{\tilde{p}_e}\tilde{\nabla}\tilde{p}_e + \frac{\chi_p}{\tilde{T}_e}\tilde{C}_e\tilde{\nabla}\psi\right)\right] = \beta\mathscr{D}\tilde{w}_e \quad (2)$$

Electron Energy

$$(\beta\,Re\,Sc_i)\tilde{\rho}\tilde{C}_e\tilde{\mathbf{u}}\cdot\tilde{\nabla}\tilde{H}_e - \tilde{\rho}\tilde{D}_e\tilde{C}_e\left(\frac{1}{\tilde{p}_e}\tilde{\nabla}p_e + \frac{\chi_p}{\tilde{T}_e}\tilde{\nabla}\psi\right)\cdot\nabla H_e =$$
$$\left(\frac{K_{eh}T_e}{\rho C_e D_e H_e}\right)_o\tilde{\nabla}(\tilde{K}_{eh}\tilde{\nabla}\tilde{T}_e) - \mathscr{D}\beta_\infty\tilde{w}_e + \mathscr{D}_e\beta\tilde{w}_{eh} \quad (3)$$

Electric Potential

$$\chi_p\left(\frac{\lambda_{D_o}}{L}\right)^2\tilde{\nabla}^2\psi = \tilde{\rho}(\tilde{C}_i - \tilde{C}_e) \quad (4)$$

In addition to these parameters, there are, of course, the governing parameters of the neutral flowfield such as the Mach number, the specific heat ratio, Prandtl number, etc. Of these, the ratio T_o/T_w (or, equivalently, ρ_w/ρ_o) enters explicitly in Eqs. (1–4) when one carries out compressibility transformations of the boundary-layer equations.

Boundary Conditions

In general, one specifies the following set of boundary conditions. At a fully catalytic and absorbing probe surface

$$C_{e,i} = 0, \qquad \phi = \phi_p \quad \text{(specified)} \quad (5)$$

and†

$$(\rho C_e/m_e)V_e(\tfrac{5}{2}kT_e - e\phi) = K_{he}(dT_e/dy) \quad (6)$$

while far from the probe

$$C_i = C_{io},\ C_e = C_{eo}; \quad \phi = 0; \quad T_i = T_\infty,\ T_e = T_{e\infty} \quad (7)$$

Probe surface boundary conditions can be generalized to include noncatalytic or partially catalytic cases and electron or ion emission phenomena. More complete discussion on these boundary conditions is given by Burke.[1] However, a brief discussion of Eq. (6) is in order here.

The kinetic distribution of electrons in velocity space is always completely out of equilibrium within few mean-free-paths of a highly absorbent wall.[2] Therefore, the continuum concept, strictly speaking, is inapplicable there. If, however, the continuum equation, Eq. (3), is to be employed all the way to the wall, then the complete kinetic nonequilibrium of the electrons previously mentioned manifests itself as a singularity in the continuum equation at $y = 0$ as $K_{he} \to 0$. Chung[3] imposed the condition that $\partial^2 T_e/\partial y^2$ be finite at $y = 0$ on physical grounds. Equation (3) then degenerates to Eq. (6) at the wall. Since K_{he} approaches zero linearly with C_e, Eq. (6) gives a finite relationship between ϕ_w, T_{ew}, and $\partial T_e/\partial y|_w$.

Definition of Parameters

Equations (1–4) in their general form present a difficult set of elliptic equations which cannot be solved analytically. Numerical solutions for the whole set are possible but not easy to obtain.

As discussed earlier, realistic probe operating conditions often correspond to simplified forms of Eqs. (1–4) which are associated with certain asymptotic limits for one or more of the nondimensional parameters given in these equations. There is a certain amount of arbitrariness in selecting these parameters but an examination of the equations reveals several which arise naturally. It is clear from Eqs. (1) and (2) that the first term on the left represents convective effects, the second term takes into account charge carrier diffusion and the third term represents charge transport caused by mobility. The term on the right is a source term that includes ionization-recombination effect in the flow. The same is true for the electron energy equation, Eq. (3) except that the right-hand side contains electron energy conduction and thermal equilibration terms in addition to the source term. Equation (4) relates the Laplacian of the potential to the electric charge separation. One group of parameters that measures the relative importance of these physical phenomena consists of $Re\,Sc_i$, χ_p, $\mathscr{D}$, $\mathscr{D}_e$, and $\chi_p(\lambda_D/L)^2$.

The behavior of Eqs. (1–4) with respect to the convective parameter $Re\,Sc_i$ is basically the same as that of neutral flows, which is well understood. The general effects of the Damkohler numbers, $\mathscr{D}$ and $\mathscr{D}_e$, on the governing equations are again the same as that of a Damkohler number in an electrically neutral, chemically reacting flow,[3] i.e., they represent the degree of thermal and chemical nonequilibrium. However, an interesting point arises in the electron-energy equations, Eq. (3). The quantity $K_{heo}T_{eo}/(\rho_o C_{eo} D_{eo} H_{eo})$ is of order Sc_i/Pr_e, which is usually of 0(1), whereas the electron-energy source terms are multiplied by $\beta \ll 1$. This is a manifestation of the fact that the electron thermal conductivity, K_{he}, is much larger as compared to the heavy gas thermal conductivity. Therefore, Eq. (3) shows that the influence of a change in the electron energy can extend through a region much greater than the species concentration and velocity boundary layers, and a much larger value of $\mathscr{D}_e$ is required to insure equilibration of T_e with the heavy-gas temperature than the value of $\mathscr{D}$ required for equilibration of the chemical reaction of ionization-recombination.

It is noted here that D_e is also very much greater than D_i. However, the distribution of electrons is closely tied to that of the ions through electric field and, therefore, the extent of the electron concentration boundary layer is usually the same as that of the ions. The electron's thermal energy, on the other hand, can be conducted to the fullest extent, dictated by K_{he}.

The basic behavior of Eqs. (1–4) can be most conveniently studied from an examination of Eq. (4). First, in the limit of $|\chi_p(\lambda_{D_o}/L)^2| \to \infty$, Eq. (4) degenerates to a Laplacian equation

* Because the degree of ionization of the gases is assumed very small, the over-all continuity, momentum, and energy equations of the plasma are essentially those of the neutral gas ($T_n = T_i$) and to first order are unaffected by the presence of the ionized species.

† Note that boundary conditions, Eqs. (5–7) are given in dimensional form.

$\tilde{\nabla}^2\psi = 0$. Equations (1–3) are then decoupled from each other which implies that arbitrary charge separation can exist, unrestricted by space-charge effects. If we define, rather arbitrarily, the "sheath" as the region where charge separation is non-negligible then the entire flow region is comprised of sheath in this case. This is then the limit of a thick sheath.

Next, let us consider the other limiting case, that of $\chi_p(\lambda_{D_\infty}/L)^2 \to 0$. We see in Eq. (4) that this limit is singular, which is evidenced by the disappearance of the highest order derivative term in that equation. As is found in all singular perturbation problems, for however small but finite the value of $\chi_p(\lambda_{D_\infty}/L)^2$, there must exist an inner region‡ (sheath) within which the left-hand side of Eq. (4) must be retained (mathematically, by an appropriate "stretching" of variables). In this sheath, the right-hand side of Eq. (4) is also non-negligible which means that the charge separation is non-negligible. In the "outer" region, where the left-hand side of Eq. (4) may be set equal to zero, charge separation is negligible, and therefore it can be identified as a quasi-neutral region in which there exist approximately equal numbers of positive and negative charges.

Obviously, the stretching parameter and, therefore, the sheath thickness are functions of $\chi_p(\lambda_{D_\infty}/L)^2$ according to Eq. (4). For the plasmas in thermal equilibrium or with assumed constant T_e/T_i the sheath thickness is mainly determined by the parameter $\chi_p(\lambda_{D_\infty}/L)^2$ provided that χ_p is of order unity. When $|\chi_p| \gg 1$, the thickness becomes a function of χ_p as well as of $\chi_p(\lambda_{D_\infty}/L)^2$, since it appears in Eqs. (1) and (2). These problems, which will be discussed in more detail subsequently, have been analyzed by the method of matched asymptotic expansions as well as by other methods.

Specific Applications to Probe Theory

The ultimate goal of probe theory is to construct probe characteristics for the various regimes previously outlined and arrive at analytic and/or empirical expressions for predicting electron number densities and temperatures in the plasma under consideration. It is evident from the above general considerations that current collection by a continuum probe of a given geometry depends on a large number of parameters. Thus, a dimensionless probe current, j, becomes, according to Eqs. (1–4)

$$j = j[(\lambda_{D_\infty}/L)^2\chi_p, \chi_p\tau, Re\,Sc_i, \mathscr{D}, \mathscr{D}_e, T_\infty/T_w] \tag{8}$$

Clearly, there exists no simple way of obtaining an explicit, general expression for the current density in this form, especially when one notes that geometry effects could play a significant role as well in the current-voltage (CV) characteristics of a probe. Historically, continuum probe theories have been developed by employing various limiting cases for one- or quasi-one-dimensional situations. These theoretical and experimental developments will be discussed briefly but systematically below, starting with the quiescent case.

1. Small Convection Limit, $Re\,Sc_i \to 0$

The simplest case is the one-dimensional, quiescent plasma limit. The earliest work in this limit was carried out for spherical and cylindrical probes by Boyd[5] and Zakharova et al.[6] An improved theoretical model for spherical probes was described by Su and Lam[7] for thin sheaths with $\mathscr{D} \to 0$ and constant properties including a constant T_e/T_i. In the limit $\chi_p(\lambda_{D_\infty}/R)^2 \to 0$,§ the exact sheath equations for spherical and elliptical probes were solved numerically by Cohen.[8–10] The Su and Lam and Cohen papers form the foundations of much further work on the subject. For example, the constant property analysis of Su and Lam[7] has been extended to cylindrical geometries by Su and Kiel,[11] and to thick sheath studies on spheres and cylinders by Kiel.[12] Extension to the case of variable properties was done by Chapkis and Baum,[13] to the nonisothermal electron temperature case by Jou and Cheng,[14] and to the case of chemical nonequilibrium by Carrier and Fendell[15] and McAssey and Yeh.[16] Further numerical work on the Su and Lam model was carried out by Cicerone and Bowhill.[17] Baum and Chapkis[18] obtained exact numerical solutions for spherical probes, for a wide range of bias potential and values of the ratio $\chi_p(\lambda_{D_\infty}/R)^2$. Recently, Bush and Fendell[19] gave a critical review of the work of Su and Lam and of Cohen, and obtained explicit results in three distinct bias potential domains for $\lambda_D/R \to 0$. The salient features of the above investigations are discussed in the following sections.

A. Frozen Chemistry, Constant Property Plasma

For the case of unbounded, quiescent, constant-property frozen-chemistry plasma, Eq. (3) is superfluous and Eqs. (1, 2, and 4) reduce to

$$\tilde{\nabla}\cdot[\tilde{\nabla}\tilde{N}_\alpha + \chi_p\tau_\alpha\tilde{N}_\alpha\tilde{\nabla}\psi] = 0, \qquad \alpha = i, e, \ldots \tag{9}$$

$$(\lambda_D/R)^2\chi_p\tilde{\nabla}^2\psi = \tilde{N}_i - \tilde{N}_e \tag{10}$$

where $\tau_\alpha = -\tau$ and 1 for $\alpha = i$ and e, respectively.

Equations (9) and (10) are still not amenable to closed formed solutions. In what have now become classic papers, Su and Lam[7] and Cohen[8] considered the thin sheath approximation for a negatively-biased spherical probe. In the work of Su analyses implies that $\tau\chi_p = 0(1)$. Nevertheless, in the work of Su and Lam attention was focused on the highly negative probe, $\chi_p \ll 0$, $\lambda_D/R \ll 1$, and $\tau = 0(1)$. Cohen considered the moderately negative probe. Both analyses were based on matched asymptotic expansions of inner (sheath) and outer (quasineutral) solutions, discussed earlier. Recently, Bush and Fendell[19] made a systematic study of the negatively biased probe in the range $1 \leqq |\chi_p| < \infty$ and obtained refinements to the studies of Su and Lam and Cohen. Current-voltage characteristics were obtained in all of these studies. For the case of equal temperatures the most accurate results of the sphere are those of Baum and Chapkis[18] who obtained exact numerical solutions to Eqs. (9) and (10) for a sphere over the entire range of $\chi_p(\lambda_{D_\infty}/R)^2$. Figure 1 exhibits the probe characteristics for positive potentials as calculated by Baum and Chapkis. The characteristics for $\chi_p < 0$ can be obtained from Fig. 1 by letting $\chi_p \to -\chi_p$, $j_i \to j_e$ and $j_e \to j_i$. For large values of R/λ_D, the probe characteristics obtained by Cohen agree well with those in Fig. 1. The agreement becomes poorer with increasing χ_p and decreasing R/λ_D.

Kiel[12] made an approximate analysis for spherical and

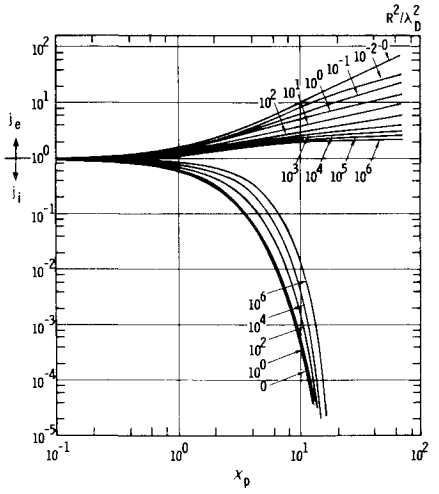

Fig. 1 Spherical probe characteristics in quiescent plasma: exact solution of Baum and Chapkis[18] [$j_{i,e} = J_{i,e}R/eD_{i,e}N_{e\infty}$].

‡ Note that here the words "inner region" are employed in a generic sense to mean the sheath. As will be discussed later, this inner region may be divided into several subregions in certain cases.

§ Here, the probe radius R is the characteristic length L.

cylindrical probes in the thick sheath limit and obtained useful results which agree to within 20% with the Baum and Chapkis numerical solution down to values of $R/\lambda_D \simeq 0(1)$ for a sphere. For example, for a sphere, Kiel obtains the following expressions for the electron or ion currents in amperes:

$$I_{e,i} = 9.73 \times 10^{-15} Z \lambda_{e,i_\infty} R R_s N_{e_\infty} (T_i + T_e)/(m_{e,i} T_{e,i})^{1/2} \quad (11)$$

where the ratio R_s of sheath radius to probe radius is given by

$$R_s = 1 + 388\{[N_{e_\infty}(T_i + T_e)]^{-1/2} |\phi_p|/R\}^{0.535} \quad (12)$$

and the units of the other quantities are N_∞ in cm^{-3}, T_o in °K, ϕ_p in volts, R and λ in cm, $m_{e,i}$ in grams.

B. Frozen Chemistry, Variable Property Plasma

Investigations that deal with probes in quiescent, variable property plasmas are fewer. The governing equations here are similar to Eqs. (10) and (11) except now the gas density and diffusion coefficients appear explicitly in the equations. In addition, one has to include the electron and heavy-gas energy equations. Chapkis and Baum[13] included the heavy-gas energy equation in the analysis of the cooled spherical probe. They neglected the electron diffusion[1,3] caused by the gradient of T_e/T_i. The electron temperature was considered to be either frozen ($T_e = \text{const}$) or in equilibrium with respect to the heavy-gas temperature. These analyses showed that the effect of the variable properties on the currents is most significant for small probe potentials. Chapkis and Baum[13] found that the thin sheath saturation current for the equilibrium electron temperature is 23% smaller than that for the constant property plasma. For the frozen electron temperature, the ion-saturation current was found to be 6% larger than that for the constant property plasma, whereas the electron saturation current was 19% smaller than that for the constant property plasma.

Jou and Cheng[14] included the electron energy equation in their analysis. Other properties, however, including the heavy-gas temperature, were considered to be constant. This analysis shows that the sheath scales are, in general, different from those given in the constant-property plasma theory.[7,8] This asymptotic analysis, however, limits the usefulness of the results to highly negative probes. This has been demonstrated by the numerical solutions of Barad and Cohen[20] who extended the Jou and Cheng results to include charge-charge collisions for strongly ionized plasmas.

C. Reacting Gas, Constant Property Plasma

There are very few studies that deal with electric probes in reacting flows, such as in flame environments. The governing equations here will now include source terms as well as a neutral particle conservation equation. The effect of the two-body ionization and three-body recombination on the probe characteristics was studied by Carrier and Fendell.[15] Either electrons or neutrals are considered as the third body in the recombination. Their results show that the ion current collected at the probe increases approximately as the square root of the Damkohler number, $\mathscr{D}$, especially when the probe potential, χ_p, becomes negative and large and if the predominant reaction is ionization. The ion current decreases when the predominant reaction is recombination. Carrier and Fendell also show that the sheath structure is affected by gas-phase reactions only when the third body is a neutral. When an electron serves as the third body for recombination, the ionization reaction is frozen.

2. Large Convection Limit, $Re\, Sc_i \gg 1$

In this limit the convective terms multiplied by the parameter $Re\, Sc_i$ in Eqs. (1) and (2) must be included in the analysis. For high-energy flows, compressibility effects are important and often transport properties show significant variations through the region under study.

The pioneering work in this area was done by Lam[21] who developed a general theory for the continuum flow of an incompressible weakly-ionized gas about an arbitrary solid body with absorbing surfaces. His analysis was limited to the thin sheath case $|\chi_p|(\lambda_{D_\infty}/L)^2 \ll 1$. Subsequently, Lam[22] and Su[23] extended Lam's work to compressible flows. More recently, Stahl and Su[24] obtained detailed CV characteristics for incompressible flow over flush-mounted, highly negative probes, in the case where the sheath is one dimensional, but thick.

The effects of nonequilibrium electron temperatures on stagnation boundary layers were analysed by Chung and Mullen.[25] The electrical characteristics of viscous shock layer including both effects of the nonequilibrium electron temperature and chemical reaction were studied by Chung.[3] Subsequently, Burke and Lam[25] and Burke[26] carried out an extensive analysis of the boundary layers in general, again, including the various effects of the nonequilibrium electron temperature and chemical reaction.

Chung and Blankenship[27,28] applied their boundary-layer analyses to the characteristics of double probes comprised of two parallel plates and of two flush-mounted probes on pointed cones. By extending these analyses and correlating the numerical results, Chung[29] derived a simple diagnostic equation for the electron number density and temperature. Denison[30] analyzed a problem similar to that of Chung[28] but for blunted cones, and obtained detailed CV characteristics in the limit of $|\chi_p|(\lambda_{D_\infty}/L)^2 \ll 1$.

Hoult[31] considered the stagnation probe mounted on sounding rockets in the limit of large $\chi_p(\lambda_{D_\infty}/L)^2$ and negligible $Re\, Sc_i$ field. Sonin[32] extended Hoult's analysis to $Re\, Sc_i \gg 1$.

In all these cases, the sheath is described by one-dimensional equations and, except for Chung,[3] the convective effects in the sheath are neglected. DeBoer and Johnson[33] and Johnson and deBoer[34] considered for the geometries of a flat plate and a cylinder aligned with the flow, the incompressible large Reynolds number case with a one-dimensional sheath, where the sheath is thicker than the boundary layer and convective effects are important.

The two-dimensional sheath was first discussed by Dukowicz,[35] who did a numerical study of the same problem for flat plates and cones using a two-dimensional Poisson equation in the limit of highly negative probe potentials. More recently, Baum and Denison[36] solved the two-dimensional Poisson equation for a flush probe in an infinite conducting surface with infinitesimally thin insulators. The most complete analysis of multidimensional sheaths has been given by Russo and Tourya[37] A number of experiments have been conducted that deal with thick sheaths in flowing plasmas. Some of these results will be discussed in the following sections.

For realistic flow situations, the incompressible, constant property case is of little interest. We will, therefore, be brief with the incompressible case and devote most of this section to compressible, variable property plasmas.

A. Incompressible, Constant Property Plasmas

Lam[21] made a detailed study of the general behavior of the governing equations. For $Re\, Sc_i \gg 1$, $|\chi_p| = 0(1)$, and large probe surfaces of order L, where L is the characteristic length of the flowfield, Lam[21] showed that the entire flowfield naturally divides itself into three regions governing the electrical characteristics. This division is controlled by the parameters Re, Sc_i, T_e/T_i, and λ_D/L.

According to Lam, the sheath thickness is of order $L(Re\, Sc_i\, T_i/T_e)^{-1/6}(\lambda_D/L)^{2/3}$, the quasi-neutral region is of order $L(Re\, Sc_i\, T_i/T_e)^{-1/2}$, and the inviscid flow region where the electric potential decays to zero is of order $L(Re\, Sc_i\, T_e/T_i)^{1/2}$. From this one can obtain a more precise definition of a thin sheath, viz.,

$$\left(\frac{1}{Sc_i}\frac{T_e}{T_i}\right)^{1/6} (Re^{1/2}\lambda_{D_\infty}/L)^{2/3} \ll 1 \quad (13)$$

when $|\chi_p|$ is of order one.

When the sheath is negligibly thin as compared to the boundary-layer thickness, the ion- and electron-saturation currents are completely governed by the quasi-neutral solutions. In fact, the first-order, "outer" solutions in the "inner-and-outer" expansions of Lam,[21] and Burke and Lam[1] are precisely the

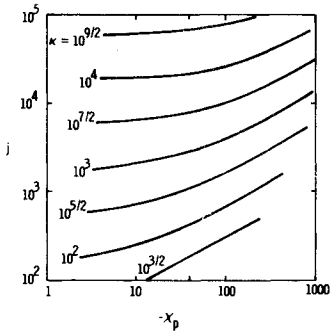

Fig. 2 Current-voltage characteristics for flowing plasma near flush probe using Blasius profile (Stahl and Su[24]) $[j_i = (J_i \kappa / eN_\infty u_\infty)(Re_x Sc_i)^{1/2}]$.

ambipolar solutions with the inner boundary conditions corresponding to the probe surface conditions. Of course, to construct complete CV characteristics, the sheath solution is necessary even if the sheath is negligibly thin as compared to boundary-layer thickness.

Following Lam,[21] Stahl and Su[24] have recently analyzed the flat-plate probe in an incompressible flow. The results of the Stahl and Su analysis shown in Fig. 2 are quite useful in that they exhibit typical CV characteristics for moderate to highly negative probes in flowing plasmas. In Fig. 2, the larger the value of the parameter κ the thinner is the sheath. With decreasing κ there is a progressively greater variation of j with χ_p. In addition, for each κ the j vs χ_p curves exhibit a relatively sudden change in slope at different values of the probe potential. This change in slope corresponds to the χ_p range where the sheath thickness λ_s becomes of the order of the boundary-layer thickness [note that $\lambda_s \propto \chi_p{}^{1/2}(\lambda_D/\delta)^{2/3}$]. A plot of j vs κ actually shows that $j \propto n_{eo}{}^p$, with $0.8 < p < 1.0$ depending on the probe bias χ_p.

It should be noted that the Stahl and Su sheath analysis is still one dimensional, even when $\lambda_s = 0(\delta)$. Recent experiments by Boyer and Touryan,[38] and two-dimensional sheath calculations by Russo and Touryan[37] indicate that the simplified analysis of Stahl and Su is indeed a good one, to within a factor of two of the more accurate estimates. (See discussion on thick sheaths later.)

B. Compressible, Variable Property Plasmas

Electrostatic probes in compressible, nonisothermal flowing plasmas present a more realistic situation, and, therefore, are more interesting than probes in incompressible flows.

The governing equations that define the probe behavior are then those given in Eqs. (1–4). For the majority of practical cases encountered in probe operation, the compressible flow investigation is limited to two-dimensional and axisymmetric boundary-layer flows. The order-of-magnitude estimate shows that the modification due to compressibility of the effect of χ_p on the electrical characteristics can be largely accommodated by considering $\chi_p(T_o/T_w)^n$, $0 < n \leqq 1$, in place of χ_p. We note from this ratio that in a compressible flow decreasing the wall temperature T_w is equivalent to increasing the applied potential χ_p, and vice versa. Probe characteristics in compressible plasmas will be discussed in thin and thick sheath limits, respectively. We examine the thin sheath first.

(i) *Thin sheath limit* $|\chi_p|(\lambda_{D\delta}/L)^2 \ll 1$

As mentioned previously, the most complete work in this regime is given by Chung et al.[3,27,29] and Burke and Lam.[1] Burke[26] extended the general methods presented by Lam[22] with special attention given to thermal nonequilibrium effects ($T_i \neq T_e$) and a detailed investigation of the role of various electron-energy transfer and exchange processes in the problem. In particular, Burke delineated four, as compared to Lam's[21] three, physically distinct regions which can differ in thickness by several orders of magnitude. The additional region for the compressible flow is the electron thermal layer defined by Eq. (3) and discussed in the Introduction. It is important to note that the asymptotic matching method cannot be applied for cases in which T_e is variable because the outer solution is dependent upon the details of the inner solution and thus upon the value of the sheath thickness in a complicated way. For this case, Burke and Lam[1] used the linearized electron-energy equation in the inner region and uncoupled the current flux from the former. A similar situation was found in the no-flow case of Jou and Cheng[14] discussed previously.

For the thin sheath case over a flat plate Burke[26] arrives at the following expression for the net current j as a function of j_i/j_e, assuming T_e is known in the quasi-neutral region:

$$j = \frac{J}{eN_{e,\delta}u_\delta}(Re_{\delta,x})^{1/2} = \frac{1}{(2Sc_i)^{1/2}}\tilde{j}_s\left(\frac{m_i}{m_e}\right)^{1/2}\frac{Q_{in}}{Q_{en}}\left(\frac{T_e}{T_i}\right)_\delta^{1/2} \tag{14}$$

where

$$\tilde{j}_s = -\beta_s\tau_s\mathscr{M}'(0)\left(\frac{T_\delta}{T_w}\right)\left(\frac{D_{e,s}}{D_{e,\delta}}\right)\left\{\frac{[1-(j_e/j_i)][1+(T_i/T_e)]_s}{1+\beta_s\tau_s(j_e/j_i)}\right\} \tag{15}$$

where $\mathscr{M}'(0)$, the normalized ion mass fraction gradient at the surface, is obtained from the solution of the ion-diffusion equation with $Sc_i = \text{const}$. Burke[25] presented a few specific results of the detailed numerical computation for Mach numbers of 2.7, 2.9, and 6 which show the ion- and electron-saturation currents for the equilibrium and frozen electron temperatures. Also, Burke and Lam[1] showed that the determination of the electron temperature at the sheath edge from the slope of the CV characteristics would involve additional terms, as compared to that collisionless plasma, which are coupled to the sheath solution itself. Because of the complexity of the problem, Burke did not propose any general diagnostic procedure based on his analysis.

Chung and his co-workers[3,4,27-29] developed a set of relatively simple diagnostic equations, based on their various analyses, which are applicable to certain flow conditions. In the analyses, the Prandtl and Schmidt numbers, and $\rho\mu/(\rho\mu)_\delta$ were assumed to be constant.

For the self-similar boundary-layer flows with frozen chemistry but equilibrium electron temperature ($T_e = T_i$), Chung[4] gives

$$j_{i,\text{sat}} = \frac{J_{i,\text{sat}}}{eN_{e\delta}u_\delta}\frac{(s/l)^{1/2}}{r^\varepsilon\mu_\delta} = \frac{0.47}{(2)^{1/2}}\left(\frac{2}{Sc_i}\right)^{2/3} \tag{16a}$$

The exponent ε is zero for the two-dimensional and one for the axisymmetric flows. Also

$$s = \int_o^x \rho_\delta u_\delta \mu_\delta r^{2\varepsilon}\,dx, \qquad l = \left(\frac{\rho_w\mu_w}{\rho_o\mu_o}\right)^{0.2} \tag{16b}$$

where the subscript o here denotes the maximum temperature in the boundary layer. Equation (16) is valid for the thin sheaths which are defined by the criterion

$$\hat{a} = 2ls\tau_\delta/(\rho_\delta u_\delta)^2 r^{2\varepsilon}\lambda_{D\delta}{}^2 \geqq 10^4 \tag{17}$$

The parameter $\hat{a}$ represents a quantity of the order of the square of the ratio of the local density-modified boundary-layer thickness to $\lambda_{D\delta}$. $\hat{a}$ is related to the Su and Stahl[24] parameter κ. Also, Eq. (17) can be shown to be comparable to Lam's[21] thin sheath criterion, Eq. (13), up to ρ_w/ρ_δ of order 10.

Equation (16) gives $N_{e\delta}$ from the measured ion-saturation current, $J_{i,\text{sat}}$, for various self-similar or highly cooled boundary-layer flows. Note that Stahl and Su[23] solution given in Fig. 2 agrees with Eq. (16a) when the criterion of Eq. 17 is satisfied and $|\chi_p| < 10$.

Chung and Blankenship,[28] using the sheath solutions of Chung,[4] analyzed approximately the flush probes located on sharp cones for the high local-Mach-number flows where the ionization takes place within the boundary layer. They assumed that the ionization reaction is confined to the narrow region about the temperature peak and that the location η_o¶ of the

¶ $\eta = \dfrac{r^\varepsilon u_\delta}{(2sl)^{1/2}}\displaystyle\int_o^y \rho\,dy$ which for cone is, $\eta = \left(\dfrac{3u_\delta}{2l\rho_\delta u_\delta x}\right)^{1/2}\displaystyle\int_o^y \rho\,dy$.

maximum of the ionized species concentration corresponds to that of the temperature peak. The expression for the peak electron number density $N_{eo} = N_e(\eta_o)$ was derived for $T_e = T_i$ as

$$N_{eo} = 1.9 \times 10^{18} Sc_i (Re_x/l)_\delta^{1/2} \frac{1}{u_\delta} \left(\frac{\rho_o}{\rho_\delta}\right) \eta_o J_{i,\text{sat}} \tag{18}$$

where N_{eo} and u_δ are in particles/cm^3 and cm/sec, respectively. $J_{i,\text{sat}}$ is the ion-saturation current in amps/cm^2.

For Prandtl number of unity, the location of the temperature peak is given by the implicit relationship

$$f'(\eta_o) = (H_\delta/u_\delta^2)[1-(H_w/H_\delta)] \tag{19}$$

where $f'(=u/u_\delta)$ is the derivative of the regular Blasius function whose tabulation is found in most of the fluid mechanics textbooks, and H is the total stagnation enthalpy. Equation (19) gives $\eta_o \approx 1$ for $H_w/H_\delta \ll 1$.

Denison[30] carried out a more detailed analysis of a similar problem but for a slightly blunted cone. In this study, he considered that the ionization takes place across the bow shock at the stagnation region of the blunted cone. The ionized species then diffuse toward the wall as they flow around the nose and along the cone in a chemically frozen state. He obtained a result very similar to Eq. (18). In fact, for slightly blunted cones, the maximum electron concentration exists at $\eta \simeq 2$, when the electrons are generated at the nose cap only. Remembering that η_o in the Chung and Blankenship[28] analysis is simply the position of the maximum ionized-species concentration, a substitution of $\eta_o = 2$ into Eq. (18) gives a value of N_{eo} for the slightly blunted cone which agrees with Denison's exact solution, within about 3%.

For the cases of frozen electron temperature and frozen chemical reaction Chung[3] and Burke and Lam[1] showed that the electron temperature varies little through the quasi-neutral region. Hence, the ratio T_e/T_i is very high near the wall when the wall is strongly cooled in a high-energy flow. Because of the large T_e/T_i near the wall Eq. (17) is no longer a valid criterion for the existence of a "negligibly thin" sheath. What is more important than the actual thickness of the sheath is that the sheath plays a much greater role in determining the ion-saturation current when the electron temperature is frozen than when it is in equilibrium, even when the physical thickness of the sheath is negligible.

For the self-similar boundary-layer flows with frozen chemistry and electron temperature, Chung and Blankenship[27,29] give the following equation obtained by correlating the numerical results for $\hat{a}$ between 10^4 and 10^9 within an accuracy of 20%. This equation is valid for highly cooled low-local Mach number flows ($M_\delta < 2$).

$$j_{i,\text{sat}} = \frac{J_{i,\text{sat}}}{eN_{e\delta}u_\delta} \frac{(s/l)^{1/2}}{r^k \mu_\delta} = \left[1 + \frac{T_e}{T_i}\right]_\delta \frac{(0.293 + 0.181 Sc_i)}{2Sc_i} \tag{20}$$

Equation (20) gives $N_{e\delta}$ in terms of the measured ion-saturation current $J_{i,\text{sat}}$ provided that $(T_e/T_i)_\delta$ is known.

By analyzing their solutions, Chung et al.[27,29] proposed that the CV relationship for a double-probe be employed to determine the electron temperature of the inviscid plasma by the relationship

$$\chi_{p,s} = 2.1(T_e/T_i)_\delta \tag{21}$$

where $\chi_{p,s}$ is $|e(\phi_{p,a'} - \phi_{p,b})/(kT_{i\delta})|$** shown on Fig. 2, part 1. Once $(T_e/T_i)_\delta$ is determined by Eq. (21), Eq. (20) can be employed to determine $N_{e\delta}$. Equations (16) and (20) hold for all similar highly cooled boundary layers on single or double probes. Also, the ion-saturation current density for the double probes is the same as that for the single probes provided that the maximum ion concentration is at the boundary-layer edge for both cases. Equation (21) should be applicable to the single probe also provided that the CV relation between the floating and the ion saturation potentials are employed.

Scharfman and Bredfeldt[39] have performed extensive electrostatic probe measurements. The experiments were conducted in a shock tube on flush-mounted probes in the range of $10^9 < N_{e\delta} < 10^{14}$ per cm^3 and $-90 < \phi_p < -3$ v. These showed that the experiments agree with Eq. (20) very closely for $\phi_p = -3$ v which corresponds to $e|\phi_p|/(kT_{e\delta})$ of 14. For ϕ_p of -15 v and -90 v corresponding to $e|\phi_p|/(kT_{e\delta})$ of 50 and 280, respectively, the experimental data deviated from Eq. (20) by factors of 2 and about 6, respectively, because of the continuous thickening of the sheath beyond the "saturation" discussed in the Introduction, part 1.

Thompson[40] simulated re-entry boundary layers and correlated flush-mounted probe data with microwave measurements. The results showed that the probe measurements as interpreted by Chung's[29] theory agreed with the microwave measurements within the experimental data scatter.

Huggins[41] and Hayes and Rotman[42] report free-flight measurements where continuum probes were employed. Although no precise examination of the theories can be made from the free-flight tests, Huggins' measurements seem to show that Eq. (16) and the theory of Kiel[12] predict the electron number densities satisfactorily.

It should be noted that all the boundary-layer theories discussed thus far assume that the convection is negligible within the sheath. Also, these theories consider that the ambipolar boundary layer is at least "locally similar" and that the sheath is one dimensional. Neglecting convection within the sheath should be quite acceptable when the sheath is much thinner than the boundary layer. Furthermore, the abovementioned approximations regarding the ambipolar and sheath regions should also be acceptable if the probe surface dimensions are sufficiently greater than the boundary-layer thickness and the sheath remains thinner than the boundary layer. As the probe surface dimensions become of the order of or smaller than the boundary-layer thickness, and the sheath becomes of the order of the boundary-layer thickness, the multidimensional aspects of the problem must be considered. We address this question in the following section.

(ii) Thick sheaths

As in the quiescent plasma case, thick sheaths occur when $|\chi_p|(\lambda_{D\delta}/L)^2$ is large either because of low electron number density or large applied potentials. For $Re\,Sc_i \gg 1$, in addition to the probe size effects, convective effects in the sheath become important.

When the sheath thickness is of the order of or greater than the probe surface dimensions and comparable to the boundary-layer thickness, the Poisson equation, Eq. (4), becomes two dimensional and, therefore, elliptic in character. Baum and Denison[36] solved numerically the nonlocally similar, compressible boundary-layer equations for a conical probe using the two-dimensional Poisson equation. Their analysis indicates that the simple one-dimensional sheath limit is valid when

$$|\chi_p| \ll 0.005[Lt/\lambda_D^2(Re)^{1/2}] \tag{22}$$

where t is the length of the probe surface.

The most complete analysis to date on thick sheaths is due to Russo and Touryan[37] who obtained numerical solutions to Eqs. (1, 2, and 4) in two dimensions, including finite rate chemistry. The electron-energy equation was not used, and therefore the ratio T_e/T_i must be specified throughout the flowfield. Special attention is paid to the boundary condition imposed on the electric potential. For example, in a two-dimensional flow problem the outer solution is obtained by a superposition of the three-dimensional Laplace equation and a contribution from the charge density above the surface. This condition has been improperly posed by Dukowicz[35] and approximately satisfied by Baum and Denison.[36] Because of its general nature, the previously mentioned analysis is capable of handling convective effects in the sheath as well as small probe size effects at all probe potentials. A typical three-dimensional contour plot of the charged particle densities obtained from Ref. 37 is shown in Fig. 3.

To supplement the above numerical studies, extensive series of experiments were conducted by Boyer and Touryan[38] in a

** a' is where the broken lines meet.

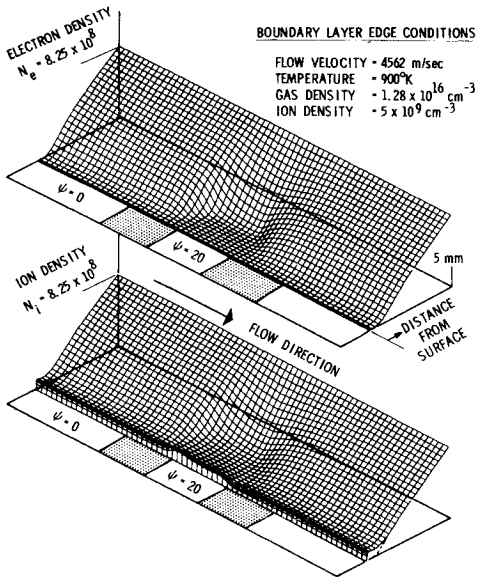

Fig. 3 Three-dimensional contour plots of charged-particle densities on flush probe at −20v bias (calculated by Russo[37]).

hypersonic shock tunnel using flush-mounted electrostatic probes on a sharp flat plate. The effects of probe size, geometry, position, bias, and local flow properties were explored. A correlation was obtained which relates current density to flow Reynolds number (based on distance from leading edge) electron convective flux, probe size, R, applied potential, and electron-to-ion temperature ratio as follows:

$$\frac{J_i(Sc_i\,Re_{x\delta})^{1/2}}{N_{e\delta}\,eu_\delta} = \text{const}\left(\frac{\lambda_D}{R}\right)_\delta^q (-\chi_p)^m \left(1+\frac{T_e}{T_i}\right)_\delta \qquad (23)$$

where

$$0.20 \leqq q \leqq 0.50; \quad m = [1+4\ln(1+0.5\kappa)]^{-1} \simeq 0.5$$

Figure 4 exhibits the data obtained by Boyer and Touryan[38] on which this correlation is based. Figure 4 also shows data from similar tests conducted by Lederman and Avidor,[43] data from Burke,[26] and some results from Scharfman and Bredfeldt.[39] Note how the data depend on $Re^{-1/2}$ as predicted by theory[1] but that the applied bias ϕ_p and the probe size enter as important parameters when the ratio $R/\lambda_D < 10^4$. Also one should note the difference between the shock tube and shock tunnel data. The former are consistently higher than the latter because of near equilibrium conditions (ionization chemistry) in shock tube boundary layers.

Thick sheath experiments have been conducted also by French, Hayami et al.[44] with spherical probes in a pressure-driven shock tube, and by Scharfman and Hammitt[45] for conical probes. The range of parameters covered in the French et al. tests were $1.1 \leqq M \leqq 1.4$; $4 < Re < 10^4$, $10^{-2} < \lambda_{D\delta}/R < 0.15$, and $-100 < \chi_p < -4$. The data can be correlated with the relation

$$(J_i R/N_{eo}\,eD_{io}) = (-\chi_p)^m(1.2+0.18\,Re) \qquad (24)$$

where

$$m = [1+0.61\ln(1+R/\lambda_D)]^{-1}$$

In these experiments the sheath was large compared to the boundary-layer thickness, except at low Reynolds numbers, and comparable with the probe radius. Consequently, agreement of the French et al.[44] data with the Su and Lam[7] theory, in the limit $Re \to 0$, is much better than agreement with Lam's theory[21] for $Re \gg 1$. In fact, for $\lambda_D/R \to 0$ Lam[21] and Chung[4,18] predict $J_i \propto Re^{-1/2}$, whereas Eq. (24) extrapolates to $J_i = 0.09\,Re^{1.0}$.

On the other hand, the thick sheath theory of Baum and Denison[36] lies within the data band of Scharfman and Hammitt.[45] However, the former predicts a slope, with the parameter κ (see Fig. 2), considerably less than that indicated by the experiments.

3. The Collisionless Thin Sheath (Dense Case)

As was stated in the Introduction, the collisionless thin sheath case arises when $L \gg \lambda \geqq \lambda_D$, and this ordering of characteristic lengths results in the condition where the charged-particle motion in the bulk of the plasma is governed by continuum phenomena (diffusion, mobility), whereas in the sheath adjacent to a solid boundary, the charged-particle motion is collision-free, since the sheath thickness is small compared to the relevant mean-free-paths.

This case was first analyzed, for a flow situation by Talbot[46] in reference to the use of a stagnation-point Langmuir probe for the determination of the freestream charged-particle density. An improved analysis for this problem was given by Brundin and Talbot.[47] The most recent study of this case is that of Tseng and Talbot,[48] who carried out a combined theoretical and experimental study of the charged-particle density and electron temperature distributions in a flat plate laminar boundary-layer flow of a partially ionized gas (argon). Agreement between theory and experiment was very good thus establishing the fact that under the dense case conditions flush probe measurements

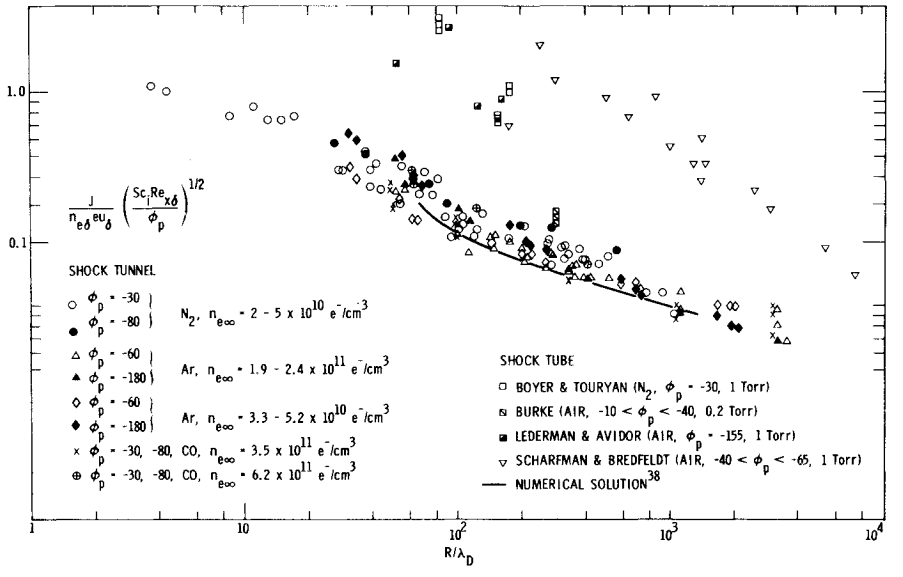

Fig. 4 Nondimensional current density on flush probe in flowing plasma as a function of the Debye ratio. A composite plot (from Boyer and Touryan[38]).

can be used to determine the charged-particle density at the boundary-layer edge.

4. Probe Surface Phenomena

In our discussion of electric probes thus far we have dealt almost exclusively with cold conductors that have fully catalytic surfaces. On such surfaces, all positive ions immediately recombine with electrons and the neutralized species then return to the plasma leaving a negligible concentration of ionized species on the surface.

On a probe surface which is not fully catalytic, the recombination process is not immediate as compared to the rates at which the ionized species arrive at the surface. Therefore, depending on the relative rates of recombination, ionized species transport, etc., non-negligible concentrations of ions and electrons exist at the surface. These concentrations are not known a priori but must result from a solution of the plasma equations satisfying the nonequilibrium surface kinetic relationship. No systematic studies are available that deal with surface layer phenomena, either theoretical or experimental.

Two of the more important effects of surface phenomena on the probe characteristics for which some results exist are surface deposit layers and electron emission.

A. Surface Deposit Layers

Surface contamination has a drastic effect on the saturation currents collected by the probe as well as on the shape of the CV characteristics. High conductivity plasmas ($N_e \geqq 10^{13}\,\mathrm{cm}^{-3}$) are specially susceptible to insulating deposits which can cause a decrease in the slope of the CV characteristics, thus leading to erroneously large T_e values. A partially catalytic or a non-catalytic surface would have the same effect on saturation currents as insulating deposit films.[1]

A method which has been found useful in minimizing the effects of contamination is to maintain the probe at a large negative potential, of the order of 100–200 v, and superimposing on it a voltage pulse which carries the probe voltage through the range of the characteristic. The large negative voltage produces sufficiently energetic ion bombardment of the probe surface to sputter off contaminants, thus providing a clean surface prior to recording the probe characteristic. This technique has been used by many investigators, and it is discussed in some detail by Swift and Schwar.[49]

B. Effect of Electron-Emission

Emission of electrons could greatly perturb the potential distribution in the neighborhood of an electrostatic probe and so invalidate theories that do not take emission currents into account. This can be due to thermionic emission in the case of hot probes or secondary emission resulting from ion bombardment. A number of studies[50] are available that deal with electron emission from probe surfaces, but the work of Chang and Bienkowski[50] is by far the most systematic and complete. They treat the case of a spherical emitting probe in the collisionless, transitional and dense regimes. Their results show a sharp increase in apparent ion-saturation current to the probe by emitted electrons escaping into the plasma. For the collisionless and transitional regimes the electron emission is space-charge limited. For the dense case, the electron emission is both space-charge and diffusion limited. Chang and Bienkowski give detailed studies of the sheath structure for the space-charge limited emission and offer guidelines for interpreting the CV characteristics in the presence of both secondary and thermionic electron emission.

5. Turbulent Plasmas

Because of the complexities of the problems, the published works on the subject of electrostatic probe diagnostics of turbulent plasmas are very few. Also, the status of the diagnostic theory is at a very preliminary stage. This is more so for the continuum probes than for the collisionless probes. Because of space limitations we will be unable to say more than just a few words on probe response to turbulent plasmas.

For the probes operating in collisionless regimes, the instantaneous mechanisms of collecting or repelling the ionized species are generally independent of the turbulence properties of the neutral gas. Hence, the only basic difference between the turbulent and laminar probe theories is that the former must now consider the unsteady boundary conditions imposed at the sheath edge (freestream) as compared to the steady boundary conditions in the laminar case. This, however, is not to say that it is a simple problem to analyze. The complexity arises from the fact that the unsteady conditions imposed by the freestream are random conditions requiring stochastic analyses. Of course, these random conditions of the ionized species are closely tied to those of the neutral gas. In addition, one should note that the unsteady response of the probe to the fluctuations of the freestream plasma is instantaneous provided that the fluctuation frequency of the plasma is below a critical frequency which is somewhat less than the ion plasma frequency.

In most engineering flow systems, the important frequencies associated with the hydrodynamic turbulence are much lower than the plasma frequency. Taking advantage of this fact and the fact that the instantaneous electron and ion transport mechanisms are unaffected by turbulence, Demetriades and Doughman,[51] Peterson,[52] Sutton,[53] and Peterson and Talbot[54] have analyzed the probe response to the turbulent plasma stream aligned in the flow direction by the use of the available instantaneous steady-state probe solutions.

Demetriades and Doughman considered the orbital motion limited case $\lambda_D/R \gg 1$; Peterson and Talbot employed both single and double probes in the regime $0.01 \leqq \lambda_D/R \leqq 0.2$ where they used the steady-state solutions of Laframboise,[55] and Sutton[53] examined the ballistic range conditions which would render the collisionless theories valid from the practical viewpoint. These investigations indicate that the mean-square fluctuation of the electron-saturation current measured at the probe is a direct measure of the mean-square fluctuation of the electron density in the freestream.

For the probes operating in continuum regimes, the instantaneous mechanisms of the electron and ion transports as well as those of the electron and ion energies are directly coupled to the turbulence properties of the neutral gas in the viscous layer. Therefore, the difference between the continuum turbulent and laminar probe theories is more fundamental than that for the collisionless probes. One case of probe response in continuum turbulent flow for which results have been obtained relating the measured mean values of the ion-saturation current to the mean electron concentration at the boundary-layer edge is the case where the sheath is embedded within the laminar sublayer. For this problem, it is only necessary to determine the mean quasi-neutral concentration profiles of the ionized species for the given turbulent boundary layer. In the potential region wherein the electron current is non-negligible such simple analysis is not sufficient.

Attempts are being made[56] to conduct statistical spectrum analyses in weakly turbulent continuum plasmas to better describe the fluctuating properties of charged particle densities. For a comprehensive review of probes in turbulent plasmas, the reader is referred to Ref. 57, Chap. 5.

6. Summary

The governing parameters and basic behavior of the steady-state continuum probes are well established for the probes consisting of perfect conductors when there are no surface emissions and fluid turbulence.

The present status of the solutions is such that the electron density and temperature at the edge of the diffusion layer can be determined from the ion-saturation current and from the current-voltage sweep between the floating and ion-saturation

potentials provided that certain conditions are satisfied. Most efforts have been directed toward analyzing the characteristics of the spherical probe in quiescent plasma and the probe in a plasma boundary layer. The status of these solutions as a presently usable diagnostic tool will be summarized briefly below.

A. Spherical Probe in Quiescent Plasma

Detailed analyses of the probe characteristics are available for the constant property plasmas. In practice, however, a considerable cooling of the heavy gas and the corresponding variation of the plasma properties take place through the diffusion layer. No general solutions of the variable property plasma are available which can be employed for the diagnostic purpose. For $T_e = T_i$, however, the constant property solutions of the ion-saturation current can be employed to determine the electron concentration of the undisturbed plasma, $N_{e,\infty}$, if the chemical reactions involving the ionized species are frozen and if the sheath is thin. This is because the governing equations of the variable property plasma can be transformed into those of the constant property plasma by assuming that $\rho\mu$ is constant.

This transformation results in the solution for the dimensionless ion-saturation current, $j_{i,\text{sat}}$, for the variable-property plasma which is the same as that for the constant-property plasma except that the D_i appearing in the definition of $j_{i,\text{sat}}$ (see Fig. 1) is changed to $D_{i,\infty}l$ where l is given by Eq. (16b). Of course the value of χ_p, at which the saturation is attained, varies, but this is unimportant. According to the Baum and Chapkis solution[18] given in Fig. 1, the ion saturation is attained at $\chi_p \simeq -10$ for $(R/\lambda_{D,\infty})^2 \gtrsim 10^3$, and $j_{i,\text{sat}}$ is a little above 2. The saturation point and the value of the saturation current are more clearly recognizable if the CV relationship is plotted on a linear or semilog scale as explained in the Introduction of part 1.

As it will be explained subsequently, $j_{i,\text{sat}}$ for the plasma boundary layer with the frozen T_e is only about 10% below that with the equilibrium T_e when $T_{e,\delta} = T_{i,\delta}$. It is logical to assume that such is also the case in a quiescent plasma. Therefore, the $j_{i,\text{sat}}$ for the constant property plasma with $T_e = T_i$ can be employed to determine $N_{e,\infty}$ for both equilibrium and frozen electron temperatures provided that $T_{e,\infty} = T_{i,\infty}$.

When $T_{e,\infty} \neq T_{i,\infty}$, the use of the existing constant-property solutions, which among other things assume that T_e/T_i is constant, is questionable. T_e/T_i is not constant through the diffusion layer, and the use of the simple logarithmic relationship[7,8] to determine $T_{e,\infty}$ cannot be substantiated.

For the thick sheaths with non-negligible $\chi_p(\lambda_{D,\infty}/R)^2$, the current for the variable-property plasma is expected to vary in the same general manner as shown by the constant-property solutions such as Fig. 1. The detailed CV relationship, however, will depend on the property variations, and use of the thick sheath solutions for the diagnostics is not a simple matter.

B. Flowing Plasma: Probes Large Relative to Boundary-Layer Thickness

General and correlated solutions are available which can be employed to determine the $N_{e,\delta}$ and $T_{e,\delta}$ when the chemical reactions involving the ionized species are frozen in the boundary layer, and the conditions of Eq. (17) are satisfied.

When $T_e = T_i$, Eq. (16a) can be used to determine $N_{e,\delta}$ from the measured saturation current for the two-dimensional and axisymmetric boundary layers.

When the electron temperature is frozen with respect to the ion temperature in the boundary layer, Eqs. (20) and (21) may be used to determine $T_{e,\delta}$ and $N_{e,\delta}$. The current-voltage sweep as well as the ion-saturation current are needed to determine these values when $T_{e,\delta} \neq T_{i,\delta}$. Equation (20) is again applicable to the types of the boundary layers for which Eq. (16a) is applicable, except that it is now required that M_δ be small. Equation (20) is constructed by correlating the various numerical solutions, and, therefore, it is not as accurate as Eq. (16a).

When $T_{e,\delta} = T_{i,\delta}$, Eq. (20) for the frozen T_e gives $j_{i,\text{sat}}$ which is about 10% below those for equilibrium T_e given by Eq. (16a). For $(T_e/T_i)_\delta \gg 1$, on the other hand, $j_{i,\text{sat}}$ given by Eq. (20) increases linearly with $(T_e/T_i)_\delta$.

When the peak electron concentration is within the diffusion boundary layer, and when it can be assumed that the chemical reaction is frozen between the peak and the probe, an equation such as Eq. (18) can be constructed[27] from Eq. (16a) to determine the peak concentration when $T_e = T_i$. Equation (18) is for the boundary layer over a cone. However, such equations can be readily constructed for any boundary layers to which Eq. (16a) is applicable. Relationships such as Eq. (18) can be employed to determine the peak electron concentration in certain chemically reacting boundary layers.

C. Flowing Plasmas: Probes Small Relative to Boundary-Layer Thickness

A few specific solutions have been obtained, but no general solution is available which can be employed for the determination of $N_{e,\delta}$ and $T_{e,\delta}$. The correlation of the various flat-plate experimental data shown on Fig. 4, guided by the solutions of Russo and Touryan,[38] gave Eq. (23). Until further analyses become available, one may, for instance, write Eq. (23) in the following explicit form

$$\frac{J_{i,\text{sat}}}{eN_{e,\delta}u_\delta}(Re_{x,\delta})^{1/2} = (1.75)(\lambda_{D,\delta}/R)^{0.4}(\chi_p/Sc_i)^{0.5} \tag{25}$$

One may, guided by the known general behavior of the boundary layers, put Eq. (25) into the following form applicable to the more general class of the boundary layers for which Eq. (16a) is valid.

$$\frac{J_{i,\text{sat}}}{eN_{e,\delta}N_{e,\delta}}\frac{(s/l)^{1/2}}{r^e\mu_\delta} = (1.75)(\lambda_{D,\delta}/R)^{0.4}(\chi_p/Sc_i)^{0.5} \tag{26}$$

Equation (26) is only an extrapolation of Eq. (25), and its validity is not substantiated.

D. Classical Space-Charge Sheath Equation

The classical, high-pressure sheath equation, the diode equation, along with the ion thermal-current expression is at times employed[39,42] for probe data reduction. The basic shortcomings of such an approach are as follows: 1) It neglects the partial-pressure diffusion of the charged particles. 2) It assumes that the ion current to the probe is given by the ion thermal current at the sheath edge. 3) Usually, no logical attempt is made to match the sheath solution to the quasi-neutral region. These approximations cannot be justified in view of the present understanding of the continuum plasma characteristics.

For sufficiently thin sheaths, the ion-saturation current is largely, if not entirely, governed by the quasi-neutral diffusion layer. Therefore, whatever the sheath theory one uses, sufficiently accurate values of $N_{e,\delta}$ should be obtainable provided that the quasi-neutral region is analyzed correctly.

Scharfman and Bredfeldt[39] employed both the simple theory based on the diode equation and Eq. (20). For the case of $\chi_p = 0(1)$, wherein the sheath was thought to be thin, the diode-theory gave the values of $N_{e,\delta}$ which differed from their experimental values by factors of 2–3, whereas Eq. (20) agreed very closely with the experimental results.†† This disagreement of the diode theory is evidently due to the fact that the three previously mentioned approximations associated with the diode theory were in contradiction to the correct description of the quasi-neutral region.

For the larger values of χ_p producing thick sheaths, the diode theory[39] gave the variations of j_i with respect to χ_p which are much faster (by several factors) than those predicted by the continuum solution of Stahl and Su[23] given in Fig. 2. Although the Stahl and Su solution is for the constant-property plasma, it is rather doubtful that the compressibility is responsible for the large difference.

†† These comparisons are given in the SRI report version of Ref. 39.

E. Use of the Electron Saturation Current for Diagnostics

According to the constant-property plasma theory,[7,8,20] there exists an electron-saturation current similar to the ion-saturation current. Therefore, in principle it should be possible to use the electron-saturation current, as well as the ion-saturation current, to determine $N_{e,\delta}$. In practice, however, the electron-saturation current is not as clearly observed as the ion-saturation current, and its relation to the electron density is rather complicated.[1,3]

Chung[3] argues that as the probe surface becomes biased to draw more electron than ion current, the positive potential is generated outside of the diffusion layer to satisfy this current bias. This positive potential heats the incoming electrons in the inviscid region, and it increases the electron pressure and mobility which results in the increased electron diffusion to the probe surface. The greater electron current to the probe, in turn, requires a greater positive potential in the inviscid region. Thus, a positive probe potential results in an amplified disturbance of the inviscid plasma, via the electron temperature, whose electron concentration and temperature one wishes to diagnose. This disturbance is quite far reaching because of the extremely high electron thermal conductivity.

Because of the large electrical disturbance of the plasma by the probe itself, considerable anomalies are associated with the relationship between the electron current and the plasma properties.

References

[1] Burke, A. F. and Lam, S. H., "A General Theory of Weakly Ionized Gas Flows Including Compressibility and Electron Energy Effects," AIAA Paper 67-100, New York, 1967.

[2] Chung, P. M., "Near Surface Electron Temperature of Weakly Ionized Plasma According to Kinetic Theory," *Physics of Fluids*, Vol. 12, No. 8, Aug. 1969, pp. 1623–1634.

[3] Chung, P. M., "Weakly Ionized Nonequilibrium Viscous Shock Layer and Electrostatic Probe Characteristics," *AIAA Journal*, Vol. 3, No. 5, May 1965, pp. 817–825.

[4] Chung, P. M., "Electrical Characteristics of Couette and Stagnation Boundary-Layer Flows of Weakly Ionized Gases," *Physics of Fluids*, Vol. 7, No. 1, Jan. 1964, pp. 110–120; also TDR-169(3230-12) TN-2, Oct. 1962, Aerospace Corp., San Bernardino, Calif.

[5] Boyd, R. L. F., "The Mechanism of Positive Ion Collection by a Spherical Probe in a Dense Gas," *Proceedings of the Physical Society (London)*, B64, Sept. 1951, pp. 795–804.

[6] Zakharova, V. M., Kagan, Yu. M., Mustafin, K. S., and Pernel, V. I., "Probe Measurements at Intermediate Pressures," *Zhurnal Technicheskoi Fiziki*, Vol. 30, No. 4, April 1960, pp. 442–449; also *Soviet Physics-Technical Physics*, Vol. 5, 1960, p. 411.

[7] Su, C. H. and Lam, S. H., "Continuum Theory of Spherical Electrostatic Probes," *Physics of Fluids*, Vol. 6, No. 10, Oct. 1963, pp. 1479–1491.

[8] Cohen, I. M., "Asymptotic Theory of Spherical Electrostatic Probes in a Slightly Ionized, Collision-Dominated Gas," *Physics of Fluids*, Vol. 6, No. 10, Oct. 1963, pp. 1492–1499.

[9] Cohen, I. M., "Couette Flow of a Radiating Fluid: Optically Thick Medium," *AIAA Journal*, Vol. 5, No. 1, Jan. 1967, pp. 78–83.

[10] Cohen, I. M., "Characteristics of a Spherical Electrostatic Probe in a Bounded Plasma," *Physics of Fluids*, Vol. 13, No. 4, April 1970, pp. 889–894.

[11] Su, C. H. and Kiel, R. E., "Continuum Theory of Electrostatic Probes," *Journal of Applied Physics*, Vol. 37, No. 13, Dec. 1966, pp. 4907–4910.

[12] Kiel, R. E., "Continuum Electrostatic Probe Theory for Large Sheaths on Spheres and Cylinders," *Journal of Applied Physics*, Vol. 40, No. 9, Aug. 1969, pp. 3668–3673.

[13] Chapkis, L. R. and Baum, E., "Theory of a Cooled Spherical Electrostatic Probe in a Continuum Gas," *AIAA Journal*, Vol. 9, No. 10, Oct. 1971, pp. 1963–1968.

[14] Jou, W. H. and Cheng, S. I., "Nonisothermal Theory of an Electrostatic Probe in a Weakly Ionized Gas," *Physics of Fluids*, Vol. 14, No. 10, Oct. 1971, pp. 2144–2151.

[15] Carrier, G. F. and Fendell, F. E., "Electrostatic Probe in a Reacting Gas," *Physics of Fluids*, Vol. 13, No. 12, Dec. 1970, pp. 2966–2982.

[16] McAssey, E. V., Jr. and Yeh, H., "Electron Heat Transfer and Probe Characteristic in a Moving Non-Equilibrium Plasma," AIAA Paper 69-699, San Francisco, Calif., 1969.

[17] Cicerone, R. J. and Bowhill, S. A., "Positive Ion Collection by a Spherical Probe in a Collision-Dominated Plasma," Rept. AR-21, 1967, Aeronony Lab., Univ. of Illinois, Urbana, Ill.

[18] Baum, E. and Chapkis, R. L., "Theory of a Spherical Electrostatic Probe in a Continuum Gas: An Exact Solution," *AIAA Journal*, Vol. 8, No. 6, June 1970, pp. 1073–1077.

[19] Bush, W. B. and Fendell, F. E., "Continuum Theory of Spherical Electrostatic Probes (Frozen Chemistry)," *Journal of Plasma Physics*, Vol. 4, Pt. 2, May 1970, pp. 317–334.

[20] Barad, M. S. and Cohen, I. M., "Continuum Theory of Electrostatic Probes in a Moderately Ionized Plasma," Rept. 2281/10, July 1973, Univ. of Pennsylvania, Philadelphia, Pa.

[21] Lam, S. H., "A General Theory for the Flow of Weakly Ionized Gases," *AIAA Journal*, Vol. 2, No. 2, Feb. 1964, pp. 256–262.

[22] Lam, S. H., "Compressibility and Nonequilibrium Effects on the Response of a Langmuir Probe in a Flowing Plasma," AIAA Paper 65-543, San Francisco, Calif., 1965.

[23] Su, C. H., "Compressible Plasma Flow over a Biased Body," *AIAA Journal*, Vol. 3, No. 5, May 1965, pp. 842–848.

[24] Stahl, N. and Su, C. H., "Theory of Continuum Flush Probes," *Physics of Fluids*, Vol. 14, No. 7, July 1971, pp. 1366–1376.

[25] Chung, P. M. and Mullen, J. F., "Nonequilibrium Electron Temperature Effects in Weakly Ionized Stagnation Boundary Layers," AIAA Paper 63-161, Los Angeles, Calif., 1963.

[26] Burke, A. F., "Electric Currents to a Flat Plate in a Supersonic Ionized Flow," AIAA Paper 68-166, New York, 1968.

[27] Chung, P. M. and Blankenship, V. D., "Theory of Electrostatic Double Probe Comprised of Two Parallel Plates," *AIAA Journal*, Vol. 4, No. 3, March 1966, pp. 442–450.

[28] Chung, P. M. and Blankenship, V. D., "Approximate Analysis of an Electrostatic Probe for Electron Density Measurements on Re-Entry Vehicles," *Journal of Spacecraft and Rockets*, Vol. 3, No. 12, Dec. 1966, pp. 1715–1718.

[29] Chung, P. M., "Diagnostic Equations of Electrostatic Double Probes for Continuum Plasmas," *Journal of Spacecraft and Rockets*, Vol. 4, No. 8, Aug. 1967, pp. 1105–1107.

[30] Denison, M. R., "Analysis of Flush Electrostatic Probes for Reentry Measurements," Rept. 06488-6065-RO-00, Sept. 1967, TRW Systems, Redondo Beach, Calif.

[31] Hoult, D. P., "D-Region Probe Theory," *Journal of Geophysical Research*, Vol. 70, No. 13, July 1, 1965, pp. 3183–3187.

[32] Sonin, A. A., "Theory of Ion Collection by a Supersonic Atmospheric Sounding Rocket," *Journal of Geophysical Research*, Vol. 72, No. 17, Sept. 1967, pp. 4547–4557.

[33] deBoer, P. C. T. and Johnson, R. A., "Theory of Flat-Plate Ion-Density Probe," *Physics of Fluids*, Vol. 11, No. 4, April 1968, pp. 909–911.

[34] Johnson, R. A. and deBoer, P. C. T., "Theory of Ion Boundary Layers," *AIAA Journal*, Vol. 10, No. 5, May 1972, pp. 664–670.

[35] Dukowicz, J. K., "Conical Electrostatic Probes in a Continuum Flowing Plasma," Rept. AN-2755-Y-1, Jan. 1970, Cornell Aeronautical Lab., Buffalo, N.Y.

[36] Baum, E. and Denison, M. R., "A Two-Dimensional Theory for the Flush-Mounted Electrostatic Probe," Rept. 06488-6526-RO-00, Sept. 1971, TRW Systems, Redondo Beach, Calif.

[37] Russo, A. J. and Touryan, K. J., "Experimental and Numerical Studies of Flush Electrostatic Probes in Hypersonic Ionized Flows: II. Theory," *AIAA Journal*, Vol. 10, No. 12, Dec. 1972, pp. 1675–1678.

[38] Boyer, D. W. and Touryan, K. J., "Experimental and Numerical Studies of Flush Electrostatic Probes in Hypersonic Ionized Flows: I. Experiment," *AIAA Journal*, Vol. 10, No. 12, Dec. 1972, pp. 1667–1674.

[39] Scharfman, W. E. and Bredfeldt, H. R., "Experimental Investigation of Flush-Mounted Electrostatic Probes," *AIAA Journal*, Vol. 8, No. 4, April 1970, pp. 662–665; also SRI Project 6138 report, July 1967.

[40] Thompson, W. P., "Experimental Evaluation of Flush Electrostatic Probes for Reentry Measurements," Rept. TR-0158 (3-40-20)-4, July 1967, Aerospace Corp., El Segundo, Calif.

[41] Huggins, R. W., "Electrostatic Probe Data from Bell Sphere B09," *AIAA Journal*, Vol. 11, No. 3, March 1973, pp. 257–258.

[42] Hayes, D. T. and Rutman, W., "Microwave and Electrostatic Probe Measurements on a Blunt Re-Entry Vehicle," *AIAA Journal*, Vol. 11, No. 5, May 1973, pp. 675–683.

[43] Lederman, S. and Avidor, J., "The Application of Flush-Mounted Electrostatic Probes to Flow Diagnostics," *Israel Journal of Technology*, Vol. 9, Nos. 1–2, 1971, pp. 19–28.

[44] French, I. P., Hayami, R. A. et al., "Calibration and Use of Electrostatic Probes for Hypersonic Wake Studies," *AIAA Journal*, Vol. 8, No. 12, Dec. 1970, pp. 2207–2214.

[45] Scharfman, W. E. and Hammitt, A. G., "Experimental Determination of the Characteristics of Negatively Charged Conical Electrostatic Probes in a Supersonic Flow," *AIAA Journal*, Vol. 10, No. 4, April 1972, pp. 434–439.

[46] Talbot, L., "Theory of Langmuir Probe," *Physics of Fluids*, Vol. 3, No. 2, March–April 1960, pp. 289–298.

[47] Brundin, C. L. and Talbot, L., "The Application of Langmuir Probe Techniques to Flowing Ionized Gases," AGARD Rept. 478, Sept. 1964.

[48] Tseng, R. C. and Talbot, L., "Flat Plate Boundary-Layer Studies in a Partially Ionized Gas," *AIAA Journal*, Vol. 9, No. 7, July 1971, pp. 1365–1372.

[49] Swift, J. D. and Schwar, M. J. R., *Electric Probes for Plasma Diagnostics*, American Elsevier, New York, 1971.

[50] Chang, K. W. and Bienkowski, G., "Electrostatic Probes," *Physics of Fluids*, Vol. 13, No. 4, April 1970, pp. 902–920.

[51] Demetriades, A. and Doughman, E. L., "Langmuir Probe Diagnosis of Turbulent Plasmas," *AIAA Journal*, Vol. 4, No. 3, March 1966, pp. 451–459.

[52] Peterson, E. W., "The Response of Free Molecule Cylindrical Langmuir Probes in a Turbulent Plasma," Rept. AS-68-10, Nov. 1968, Univ. of Calif., Berkeley, Calif.

[53] Sutton, G. W., "Use of Langmuir Probes for Hypersonic Turbulent Wakes," *AIAA Journal*, Vol. 7, No. 2, Feb. 1969, pp. 193–199.

[54] Peterson, E. W., "Collisionless Electrostatic Single-Probe and Double-Probe Measurements," *AIAA Journal*, Vol. 8, No. 12, Dec. 1970, pp. 2215–2219.

[55] Laframboise, J. G., "Theory of Spherical and Cylindrical Langmuir Probes in a Collisionless, Maxwellian Plasma at Rest," UTIAS Rept. 100, June 1966, Univ. of Toronto, Toronto, Ontario, Canada.

[56] Chung, P. M. and Marcisz, T. J., "Turbulent Shear Flow of Continuum Plasma," *Proceedings of the International Symposium on Dynamics of Ionized Gases*, Tokyo, Japan, Sept. 13–17, 1971.

[57] Chung, P. M., Talbot, L., and Touryan, K. J., *Electric Probes in Stationary and Flowing Plasmas: Theory and Application*, Springer-Verlag, New York, 1974.